Use Satellite Infrared Brightness Temperature Data to Evaluate HWRF Ferrier-Aligo microphysics scheme: VERTICAL ADVECTION OF TOTAL CONDENSATE VERSUS SEPARATE HYDROMETEORS.

A report for the Developmental Testbed Center Visitor's Project.

By Shaowu Bao

Collaborators: Ligia Bernardet and Evan Kalina at GSD/NOAA and Kathryn Newman, Mrinal Biswas and Greg Thompson at NCAR

November 2018

ABSTRACT

Satellite GOES-13 IR brightness temperature data were used to evaluate HWRF's forecast of tropical cyclones (TCs) using the Ferrier Aligo (FA) microphysics scheme with the total condensate advection (operational) versus the FA scheme with separate hydrometeors advection (FA-adv). Three real-case hurricanes and an idealized one were used as the study cases. Comparing the IR brightness temperature images from the model and the observation, we found that the FA-adv method forecasted significantly larger-sized storms with a weaker maximum wind speed than the operational FA method. Besides the satellite images, this larger size and weaker maximum wind speed by FA-adv were also confirmed by other metrics such as the modeled hydrometeor fields, pressure-wind scatter plots, multi-cycle intensity statistics, and 10-m wind and MSLP patterns. The idealized HWRF TC simulation revealed that the FA-adv method produced a larger upward cloud water advection than FA. The difference in the cloud water upward advection between FA and FA-adv led to more diabatic heating in FA-adv than FA, and this difference in diabatic heating caused more angular momentum to be imported into the FA-adv vortex, thus expanding the size of its simulated storm. An analysis using the cyclostrophic balance showed that the diabatic heating radial profile causes the maximum 10-m wind to be weaker in FA-adv than FA, but in regions of the storm away from the vortex center, the surface winds are stronger in FA-adv than FA. In summary, although in theory FA-adv should be more realistic, the hurricane sizes and structures forecasted by FA agree with the observations better than those forecasted by FA-adv. It should be noted that HWRF, like other numerical weather prediction (NWP) models, is a very complex system, and the tuning in other parts of the model system could have masked the errors introduced by the total condensate advection. In this study we focused on understanding the mechanisms that are responsible for the forecasted discrepancies between FA and FA-adv, instead of seeking to improve the HWRF performance with FA-adv. Future work is needed to identify those tunings so that the separate hydrometeors advection can achieve better forecast performance.

1. INTRODUCTION

HWRF's forecast skill has steadily improved in recent years. Each year, upgrade candidates, such as those related to data assimilation techniques, physics schemes, and model resolutions, are tested by EMC and DTC using multi-season cases. These testing and evaluation (T&E) results are

assessed according to the candidates' track and intensity forecast skill statistics, to determine which candidates will be implemented in the next upgrade.

A microphysics scheme describes the processes that control the formation of cloud droplets and ice crystals, their growth, and fallout as precipitation. These processes also control the release of latent heat during phase changes. Microphysics processes modulate the thermo-dynamical structure and energy distribution of tropical cyclones. NWP model forecasts are sensitive to the choice of the microphysics scheme, which is a large source of forecast uncertainty. For hurricane forecasts, it has been demonstrated that microphysics schemes can impact hurricane track (Fovell and Su, 2007) and intensity (Pattnaik and Krishnamurti, 2007a and 2007b; Zhu and Zhang, 2006) forecasts.

Currently, the microphysics scheme used in the operational HWRF is the Ferrier-Aligo (FA) scheme (Biswas et al., 2018). It is a modified version of the original Ferrier scheme used in the ETA model (Ferrier, 2005 and 1994). These modifications enhanced representation of the storm structure and provided more realistic forecasts of the distributions of hydrometeors, especially for ice concentration and precipitation fall speeds (Biswas et al., 2018). For computation efficiency, the current FA scheme does not adopt the separate explicit advection for the multiple hydrometeor species, meaning that only the combined sum of the microphysics variables--the total condensate--is advected horizontally and vertically.

As mentioned earlier, T&E using multiple seasons' hurricane cases are conducted each year to decide which microphysics scheme candidate will be implemented for the next upgrade. For the 2017 implementation, the FA scheme with explicitly separate advection of multiple species (FA-adv) (Aligo et al., 2014) and the Thompson scheme (Skamarock et al., 2008; Thompson et al., 2008) were tested as upgrade candidates. However, DTC's and NCEP/EMC's extensive T&E results showed that neither the FA-adv nor the Thompson scheme had a conclusively satisfactory performance to warrant adoption in the 2017 upgrade. Therefore, the current FA scheme, without explicit separate advection of the hydrometeor species, remained the operational microphysics scheme for 2017.

Large T&E are critical to making sure the new upgrades will improve or at least not degrade the objective track and intensity forecast skills. However, evaluation and diagnostics activities are complex and should go beyond the track and intensity error statistics. In other words, track and intensity forecast errors alone are often not enough to reveal the strength and weakness of a physics parameterization scheme and its interaction with other physics processes. In this regard, although the T&E track and intensity results were indeed poor for FA-adv and Thompson, it may not be because the microphysics schemes are bad. Perhaps there are compensating errors somewhere else in the physics suite. Or perhaps there is an error in how the FA-adv is connected to the WRF-NMM dynamic core (this possible error is referred to hereafter as a software problem). After the HWRF 2016 upgrade, the following questions remained unanswered and therefore deserve further investigation: (1) Is there a software problem in the implementation of the explicit separate species advection in HWRF FA-adv? If yes, how can the problem be identified and fixed, (2) Suppose the software problem, if any, is fixed, will the explicitly separate species advection in FA-adv lead to more realistic modeling of the microphysics processes? (3)

How can we relate the accuracy in HWRF forecasting cloud versus the track and intensity errors and can we quantify this relationship? Answers to these questions are provided in this report.

In this report we seek to answer these questions by evaluating and diagnosing HWRF's FA and FA-adv microphysics schemes using remote sensing data as well as through detailed numerical case studies to better understand the strengths and weaknesses of these two microphysics schemes, which is helpful to reduce uncertainty and provide insight for HWRF's future improvements.

The report is organized as follows. Section 2 describes the observational data and studied cases. The HWRF model, experiment design and evaluation methods are introduced in Section 3. Results are given in Section 4 and discussion in Section 5, followed by concluding remarks.

2. OBSERVATIONAL DATA AND STUDIED CASES

The infrared (IR) brightness temperature images data from NOAA's Geostationary Operational Environmental Satellite (GOES) 13 were used to validate the model forecasts. IR brightness temperature can be used to detect the cloud structures as a cold IR brightness temperature in an area indicates the existence of cloud top and a warm one reveals non-cloud earth surface. Thus the GOES-13 data provide useful information of the hurricane's coverage and structure, especially considering the lack of conventional observational data over the ocean and during strong storms. The GOES-13 IR brightness temperature data were downloaded, processed and staged on NOAA's Jet computer using software tools developed through a previous DTC visitor project[1]. New data were obtained for three recent cases. The data were archived on HPSS and are available to the public. The studied real cases include hurricanes (1) Hermine 2016 09L August 29 to September 02, (2) Matthew 2016 14L September 29 to October 09, and (3) Jimena 2015 13E August 28 to September 07. These are all recent TCs that have been tested extensively by EMC and DTC, so the test results in this report can be compared with those results.

3. MODEL AND METHODS

HWRF v3.9a, which corresponds to the 2017 operational HWRF, was used in this study. In HWRF v3.9a, FA is the default choice of microphysics scheme, but it also has the option to use the FA-adv scheme, making it possible to run each case in parallel, using the FA and FA-adv respectively, and then make comparisons.

As mentioned above, three real TCs with multiple cycles were forecast and one idealized TC with one cycle was simulated. For each output, synthetic satellite IR brightness temperature images were generated using the Unified Post Process (UPP). UPP incorporates the Community Radiative Transfer Model (CRTM) to compute model derived brightness temperature for various instruments and channels including IR. The model derived synthetic IR brightness temperature images, from forecasts using FA and FA-adv, were then compared with the observed GOES-13 images. As mentioned earlier, the cold IR brightness temperature areas correspond to the convective cloud tops, and the warm areas indicate low-cloud or less-cloudy conditions such as

[1] *Evaluation of two HWRF microphysics/radiation configurations with remote-sensing data* by Bao, final report available at http://www.dtcenter.org/visitors/reports_2014/Bao-DTC-project-report.pdf

the earth surface. Thus by comparing their synthetic IR brightness temperature images with the observed ones, we can evaluate how well the FA and FA-adv schemes simulate the size and structure of the convection and clouds.

In addition to the visual comparison, a statistical metric, the Probability Density Function (PDF), was also used in the evaluation. The PDF function uses an IR brightness temperature image, either observed or model-derived synthetic, as input. The brightness temperature range of 180 K to 310 K was equally divided into 50 bins as X-axis values. Each of the grid points (or pixels) in the dataset was counted into one of these 50 bins based on the cloud-top brightness temperature of that grid point. In the end, the probability (in percentage %), as the ratio of the number of grid points in a bin over the total number of grid points in the entire satellite image, was calculated for all the bins and plotted as Y-axis values. The PDF function analysis provides the information about the relative amount of the high clouds (with cold cloud-top temperatures), low clouds (with less cold cloud-top temperatures) and non-clouds (warm land or ocean surface). The advantage of this non-local PDF metric is that, since the locations of the grid points are not considered in the PDF function, forecasts are not penalized by associated tracker errors.

Idealized HWRF was also used as a tool for diagnosing the behaviors of the FA and FA-adv schemes. The initial conditions for the idealized HWRF simulation are specified using an idealized prescribed vortex superposed on a base-state quiescent sounding on an f-plane at the latitude of 12.5^{o}. The sea surface temperature was time-invariant and horizontally homogeneous, with the default set to 302 K. By default, no land is used in the simulation domain, although a landfall can be simulated by choice. Using such simple and idealized environmental and initial conditions, one can isolate the processes to be studied. Although the real-case TC simulations can be compared with observations and performance skill metrics, they are sometimes difficult to analyze due to the complicated interactions of the environmental fields and the physical processes in the vortex. In this study, the idealized HWRF allowed us to concentrate on the microphysics and vertical advection processes. All the functions in the operational version of HWRF such as the triple-nested domain configuration with grid spacing at 18, 6, and 2 km, the vortex following nested grids, and all operational atmospheric physics, as well as the supported experimental physics options in HWRF, can be used in the idealized simulation. The UPP can be used to post process the idealized HWRF simulation output and the synthetic IR brightness temperature satellite images can be created.

The evaluation methods described earlier are also used for the idealized HWRF simulations. An idealized HWRF simulation, with the full physics options using the FA microphysics scheme, was run to 96 hours, so that the hydrometeor fields, i.e. cloud water, rainwater, snow, and ice, were established and the TC was a mature storm. A restart file was saved from the 96-hour simulation. From there, a series of short 20-minute idealized TC sensitivity experiments were carried out. These sensitivity experiments were short because some of the experiments used unrealistic configurations that would cause the model to crash for long simulations. In these sensitivity experiments, however, the model with these unrealistic options can still complete the short 20-minute runs and generate results that provide insight into the sensitivity of the schemes. The experiments for FA and FA-adv included: (1) no diabatic heating in microphysics scheme, (2) no

condensation in the microphysics scheme, (3) all physics schemes turned off, (4) zero cloud optical depth, (5) no radiation, and (6) no cumulus convection scheme.

4. RESULTS

In the proposal, more study cases were planned than these three. However, as the forecasts for the three cases, namely, hurricanes Hermine (2016), Matthew (2016) and Jimena (2015), consistently showed a clear signature, i.e., the FA-adv method produced larger storms than the FA method, we decided that some of the planned case studies were not necessary anymore; instead, a series of idealized HWRF simulations have been conducted to explain the mechanisms that caused the larger sizes of the simulated storms.

4.1. Software issues.

In the proposal, one task is that we identify any possible software problems in the implementation of the explicit separate species advection in HWRF FA-adv method. It was determined that the FA and FA-adv methods share the same advection and microphysics code. The only difference between the two implementations is that FA passes the total condensate to the advection routine while FA-adv passes the hydrometeors to the advection routine separately. Therefore, it is likely that the advection and microphysics routines for FA-adv do not contain software errors, and any difference between the FA and FA-adv TC forecasts can be attributed to scientific reasons rather than software problems. Also, in the T&E part of this project, all the test cases were able to run to completion without crashing. Therefore, it was concluded that there is no software-related error in the FA-adv method.

4.2. Synthetic and observed IR brightness temperature images

The most distinct difference between the FA and FA-adv results is the simulated storm size. In the images shown in Figure 1, which is a snapshot of IR brightness temperature of hurricane Hermine, the color represents the IR brightness temperature with the deep blue indicating the cold cloud top and the red-brown the warm surface with small cloud fraction. From Figure 1, one can see that FA and FA-adv forecasted similar center locations and shapes of the storm that both matched the observed. However, the FA-adv produced cloud coverage, represented by the blue and deep blue colors, that is noticeably larger than that produced by FA. FA's storm size matched the observations, but its blue color is deeper, indicating stronger convection in FA. Note that although Figure 1 only shows a snapshot of one storm, all the

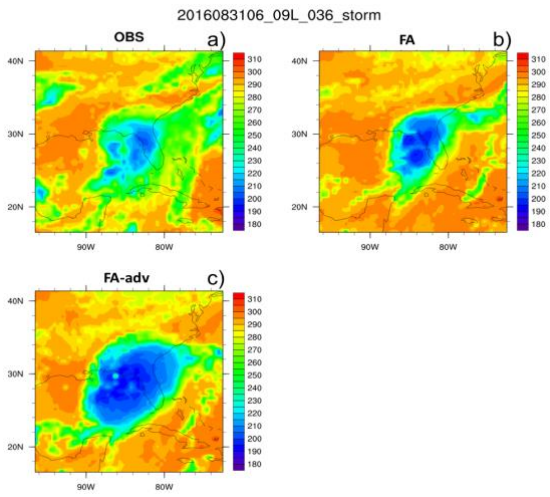

Figure 1 a snapshot of IR brightness temperature of hurricane Hermine as the 36-hour forecast in the cycle that started 06Z 08/31/2016 on the storm scale middle domain d02 (a) observed (b) FA (c) FA-adv

cases examined in this study generally produced the same result, i.e., FA-adv produces larger cloud coverage and therefore larger-sized storms than FA.

4.3. Probability density function

The PDF method, described in Section 3, also showed the larger cloud coverage in FA-adv than in FA. In Figure 2, which is from the storm-scale domain grid d02, the FA-adv has a much higher PDF (reaching 6%) on the cold side (200 K - 220 K) of the brightness temperature spectrum than the FA (reaching 4%). The FA is slightly higher than the observations, indicating a slight overestimation, but still quite comparable, of the storm size in the 2017 operational HWRF. On the warm side (280K-300K) of the IR brightness temperature spectrum, however, the FA PDF (reaching 16%) is much larger than both those of FA-adv (reaching 4%) and the observations (reaching 4%). The observations, on the other hand, have medium brightness temperature areas (230-280 K), the area covered mostly by low-cloud, which were underestimated by FA and FA-adv.

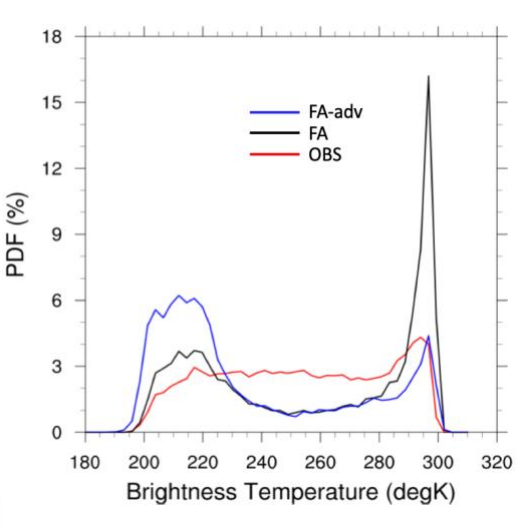

Figure 2 probability density function (PDF) of the synthetic FA, FA-adv, and the observed (OBS) IR brightness temperature

4.4. 34 kt wind and mean sea level pressure (MSLP)

TC sizes are often measured in terms of the 34 kt 10-m wind contours and the MSLP pattern. The difference between TC size produced by FA and FA-adv in terms of 10-m wind 34 kt and MSLP contours is consistent with that found in terms of IR brightness temperature. In Figure 3, the FA-adv MSLP contours (Figure 3b) span a larger distance than those for FA (Figure 3a), as if all the contours in FA-adv have been stretched outward. The minimum MSLP in FA-adv is also deeper than that in FA. For the 10-m winds, (see Figure 3c and 3d), the extent of the 34 kt contour is also wider in FA-adv than in FA. The maximum 10-m winds, however, are weaker in FA-adv than in FA. That is, FA-adv forecasted a TC that is larger but weaker for intensity measures in terms of the maximum 10-m wind. Although the minimum MSLP for FA-adv is deeper than FA, FA's MSLP contours are denser, which will be revisited in the discussion of intensity differences in Section 5.

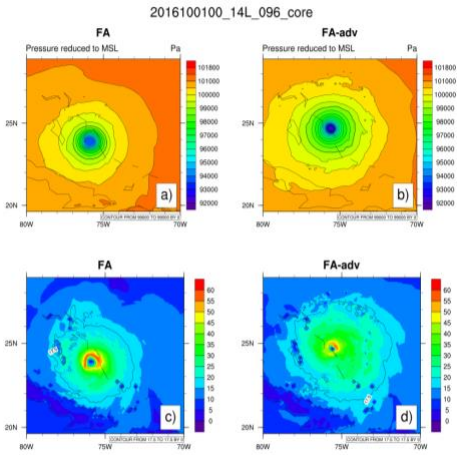

Figure 3 the MSLP of a) FA and b) ADV and the 10-m winds for c) FA and d) ADV. In c and d the black contour lines show the 34 kt wind.

The pattern of larger and weaker forecasted storms by FA-adv is also demonstrated through a comparison of the pressure-wind (P-V) relations for FA, FA-adv and Best Track (see Figure 4). The scatter plot for FA-adv contains some P-V points corresponding to deeper MSLP with weaker 10m winds then those found in the FA scatter plot, indicating some points in the FA-adv were shifted toward the low-pressure low-wind regions of the scatter plot, confirming the same pattern shown in Figure 3. The mechanisms that lead to this pattern and its implications are discussed later. When compared with the Best Track P-V plot (Figure 4 right-panel), both FA and FA-adv overestimated the deepening of the MSLP, as can be seen from the slope of the regression lines.

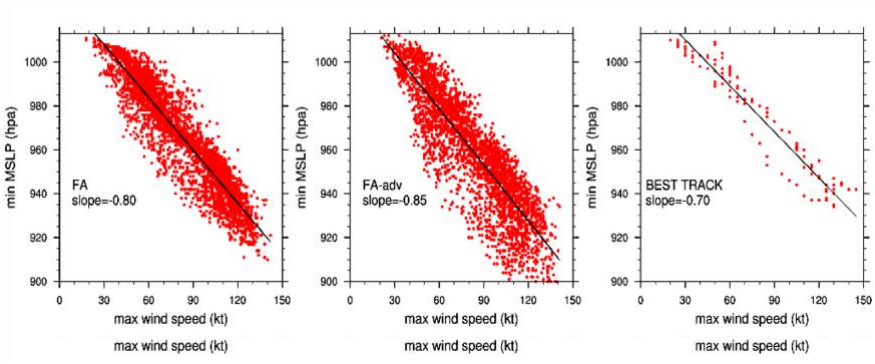

Figure 4 Pressure-wind scatter plot for FA, FA-ADV and the Best Track.

4.5. Hydrometeor fields

In addition to the IR brightness temperature images, 10m wind and MSLP, the larger storm size simulated by FA is also evident in the hydrometer contour plots (Figure 5). in Figure 5 the FA-adv generated significantly larger fields of the hydrometeors than from FA.

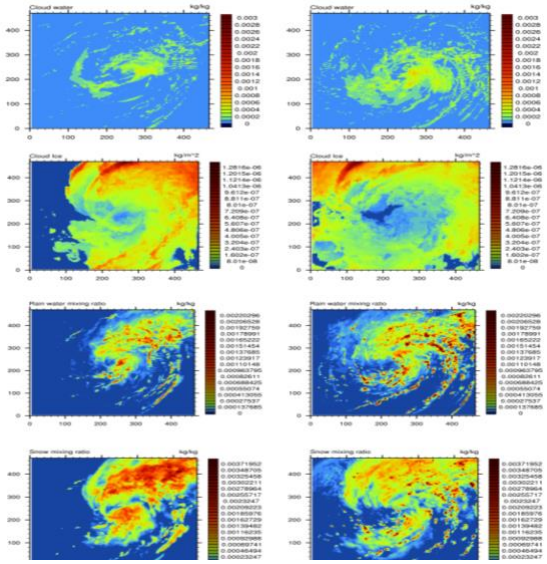

Figure 5 The shaded contours of the mixing ratios hydrometeors of cloud water (first row), ice water (second row), snow water (third row) and rainwater (fourth row), at representative isobaric levels for FA (left column) and FA-adv (right column) in the real case TC of Matthew 2016. Note the color scales for these species are different.

4.6. Cycle-forecasted Intensity statistics:

The simulated tracks between the FA and FA-adv methods were comparable (not shown), but their intensities differed significantly. Figure 6 shows the forecasted intensity of the hurricane Matthew (2016) for 19 cycles. For shorter lead times (12 hours or less), FA and FA-adv were nearly identical. This is because the hydrometeors are set to zero in the initial conditions, so there is no difference between the advection of separate hydrometeors and the total condensate. With time, minimum MSLP from FA-adv becomes deeper than that in FA, but its maximum 10-m wind becomes weaker. This is also consistent with the trends shown in Figures 3 and 4, highlighting a pattern that is seemingly contradicting the established relationship that a deeper minimum MSLP usually means a stronger TC vortex and thus stronger 10-m wind. The mechanism that caused this discrepancy is discussed in the next section.

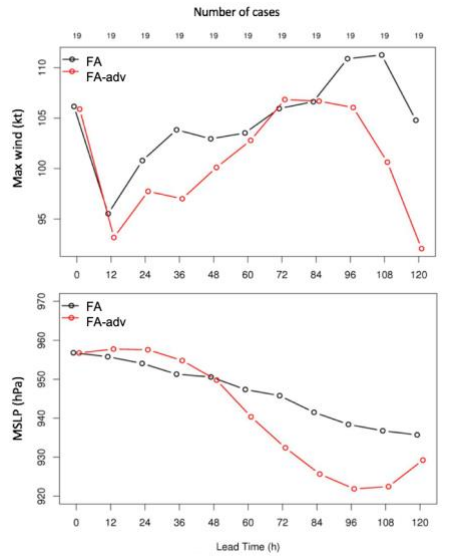

Figure 6 The maximum 10-m wind (top) and minumum MSLP (bottom) forecast for Hurricane Matthew (2016)

5. Discussion

To investigate impact the different advection methods, namely FA and FA-adv, on the simulated TC size, structure and intensity, it is necessary to review the difference between the implementations of FA and FA-adv. The schematic shown in Figure 7 illustrates the differences between the algorithms for FA-adv and FA. The same microphysics column subroutine is used by both microphysics schemes. The difference between FA-adv and FA is mainly with respect to how the advection of the hydrometeors is handled. In FA, prior to calling the advection routine, the hydrometeors are summed to form the total condensate (CWM in Figure 7) and their fractions are assumed to remain unchanged during the advection. The total condensate is advected using the vertical gradient of the total condensate, and after the advection, each hydrometeor is obtained from their respective fractions. After the advection, the new total condensate and their fractions are passed into the microphysics column routine. In FA-adv, the mixing ratios of the different hydrometeors are advected separately. The new mixing ratios after the advection are converted to the total condensate and fractions before being passed to the microphysics column

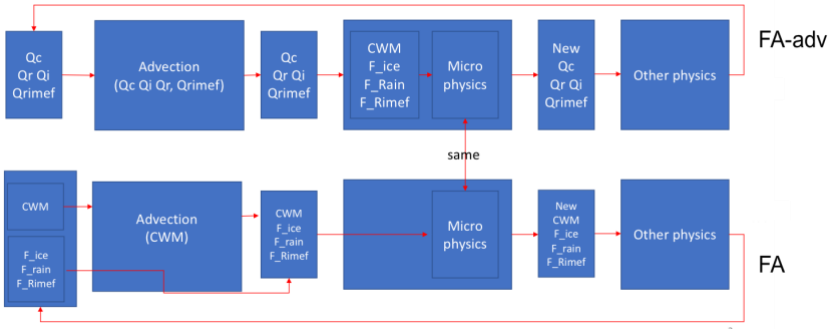

Figure 6 The schematic flow-charts of the algorithms of the FA-adv and FA

routine. However, the same microphysics column routine was used in both FA and FA-adv. Therefore, the diagnostics of the FA-adv and FA focused on the impact of advection on the hydrometeors, particularly the vertical advection.

The general formula of the rate of change of a state variable due to only vertical advection can be expressed as $\frac{\partial f}{\partial t} = -w\frac{\partial f}{\partial z}$, where the f is the variable that is advected, w is the vertical velocity, and $\frac{\partial f}{\partial z}$ is the vertical gradient of this state variable. Therefore, the vertical gradient is an important factor affecting the vertical advection of state variables. A hypothetical example can help illustrate how advecting the total condensate instead of individual hydrometeor types will lead to different distributions of the hydrometeors. Consider a setup where the total condensate varies with height, but the rainwater profile is constant with height. The separate advection method will result in a zero upward advection of rainwater; however, the total condensate advection method would produce non-zero upward advection of rainwater because the total condensate gradient is used. For this scenario, the total condensate advection in FA would overestimate the upward advection of rainwater and underestimate the upward advection of cloud water. By correcting this problem, the FA-adv, relative to FA, transports more cloud water upward, leading to relatively more ice, snow and rainwater and more diabatic heating from condensation. The relatively more diabatic heating would cause more angular momentum to be imported into the TC vortex, which would lead to FA-adv producing larger TCs than FA. In this section we use results from the sensitivity experiments to validate the hypothesis that the differences between the vertical advection of the hydrometeors led to FA-adv producing larger TCs. For simplicity and to isolate the problem from more complex interactions with the environmental factors, the idealized HWRF was used.

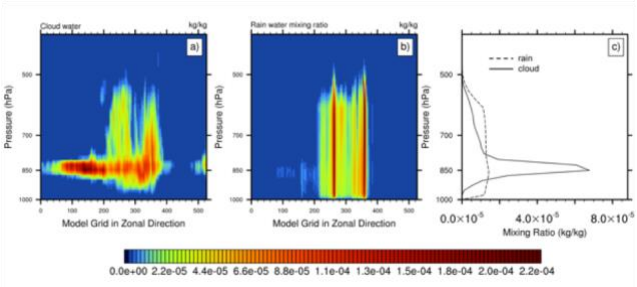

Figure 7 Meridionally-integrated mixing ratios (in kg/kg) of (a) cloud water, and (b) rainwater in the restart file of the idealized HWRF run at 96 h. (c) is the domain-averaged vertical profiles of rainwater and cloud water mixing ratio in the idealized simulation FA at 96 h.

A 96-h idealized simulation was conducted with the FA scheme. At 96 h, a mature TC was established and its hydrometeor fields were fully developed. The domain-averaged rainwater and cloud water mixing ratio vertical profiles at 96-h are shown in Fig. 8. The cloud water had a sharp spike around 850 hPa, forming a large gradient. The rainwater profile, on the other hand, was vertically uniform throughout the lower troposphere with near-zero gradient. The total condensate, which in the low levels was mostly comprised of cloud water and rainwater, had a gradient (not shown) that was between those of cloud water and rainwater. The lifting condensation level (LCL) calculated from the sounding used to initialize the idealized HWRF simulation was at 973 hPa, consistent with the cloud base shown in Fig. 8.

Since the vertical gradient of the total condensate was much larger than that of the rainwater, the rainwater's upward advection was overestimated by FA. If the rainwater had been advected individually, its uniform vertical profile would lead to very little upward advection near the 850-

hPa level. Similarly, because the gradient of the total condensate is smaller than that of the cloud water, cloud water's upward advection was under-estimated. These discrepancies were corrected when the hydrometeors were advected separately in FA-adv, and therefore more cloud water was advected upward near 850 hPa in FA-adv than FA. The larger upward advection of cloud water in FA-adv when compared to FA has implications for the simulations of the other hydrometeors as well as the dynamics when the physics schemes were turned on.

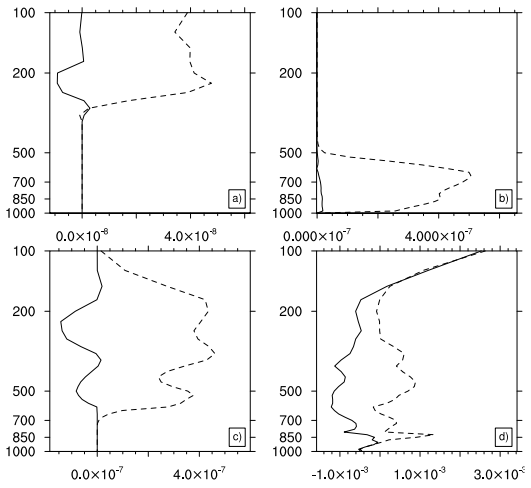

Figure 8 Domain-averaged change of the mixing ratios of (a) ice (b) rainwater (c) snow and (d) temperature during the 20-minute idealized HWRF run with full physics. Dashed lines are FA-adv and solid lines FA

The larger upward advection of cloud water associated with FA-adv will also impact the distributions of the other hydrometeors as well as the dynamics when the physics schemes are turned on. In FA-adv, more cloud water (relative to FA) particles can be carried further upward by the updraft and turn into cloud ice, which can turn into more snow and, in turn, increase the rainwater when it falls below melting altitude. In other words, this increase has the potential to impact all the microphysics processes. The larger upward advection of rainwater in FA, instead, can only fall again as rain drops. Therefore, the upward advection of more cloud water near 850 hPa in FA-adv represents a continuous source of cloud water that gets moved upward with the potential to became ice and eventually increases the mixing ratios of all of the other hydrometeors. This is clear in Figure 9 that shows the domain-averaged change in the simulated of hydrometeors of ice, rainwater, snow. In Figure 9 all the physics schemes are turned on. Note the x-axis scales in Figure 9 (a),(b) and (c) are different.

The larger cloud water advection in FA-adv (relative to FA) also leads to more diabatic heating due to condensation as water vapor is converted to cloud water near 850 hPa, as shown in Figure 9 (d).

The extra diabatic heating in FA-adv significantly affects the dynamics of the simulated TC. It is well established that a TC responds to changes in diabatic heating through changes in its secondary circulation, which imports angular momentum into the vortex. The larger diabatic heating in FA-adv leads to a stronger secondary circulation with more angular momentum being imported into the vortex, i.e., an angular momentum convergence. Angular momentum is defined as vr where the v is the tangential wind speed and r is the radial distance. The angular momentum in the real case hurricane Matthew from FA and FA-adv is shown in Figure 10, which

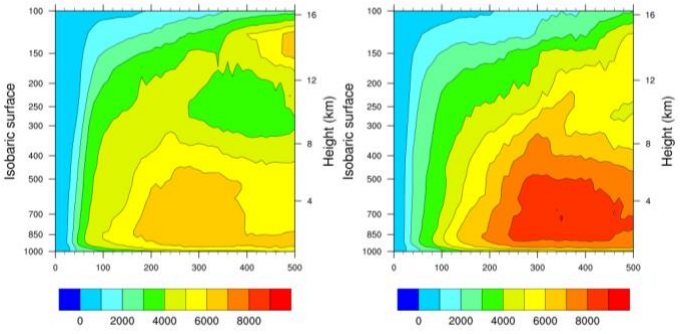

Figure 9 Pressure-radial cross-section of the azimuthally averaged angular momentum in FA (left) and FA-adv (right) for the simulation of hurricane Matthew 2016 14L 2016100100 cycle valid at 96 hr

shows that the maximum angular momentum for FA was 6000 m^2/s, while in FA-adv the maximum reached 9000 m^2/s, suggesting more angular momentum has been imported into the vortex due to the larger diabatic heating in FA-adv. However, note that the increase in angular momentum in FA-adv occurred mostly in the area further than 100 km from the vortex center. Near the vortex center, or within 100km from the vortex center, however, the angular momentum is less in FA-adv than FA. Also, the angular momentum contours in FA-adv are less dense than those in FA.

The pattern of the less-dense angular momentum contours near the vortex center in FA-adv is more evident from the tangential wind cross-section in Figure 11. The tangential wind contours from FA-adv are pushed more outward and are stronger than FA in the distance further than 100 km from the vortex center. But near the vortex, FA-adv's tangential wind is weaker than FA, which is also consistent with Figure 10. So indeed the larger diabatic heating associated with FA-adv caused more angular momentum convergence, but the increase in angular momentum is realized by expanding the size of the storm, instead of enhancing the maximum wind speed.

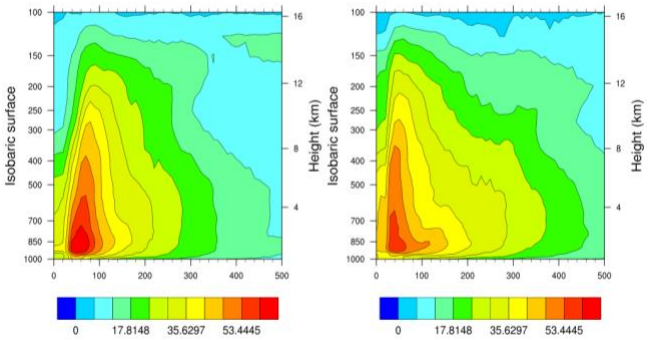

Figure 10 Pressure-radial cross-section of the azimuthally averaged tangential wind speed in FA (left) and FA-adv (right) for hurricane Matthew 2016 14L 2016100100 cycle valid at 96 hr

This seemingly paradoxical result --- the relative extra diabatic heating and deeper minimum MSLP in FA-adv accompanied by a weaker maximum wind speed --- can be explained using the cyclostrophic balance near the vortex center. Near the center of the tropical cyclone vortex, the wind and pressure approximately follow the cyclostrophic balance relation of $\frac{V^2}{r} = -\frac{1}{\rho}\frac{\partial P}{\partial r}$, where the V is the tangential wind, r is the radial distance from the center of the vortex, ρ is the air density, and $\frac{\partial P}{\partial r}$ is the pressure gradient. Since the larger diabatic heating in FA-adv caused a pressure adjustment and deepened the MSLP, it changed the pressure gradient $\frac{\partial P}{\partial r}$ and the change of the tangential wind V can be approximately decided by $V = \sqrt{(-\frac{r}{\rho}\frac{\partial P}{\partial r})}$ derived from the cyclostrophic relation.

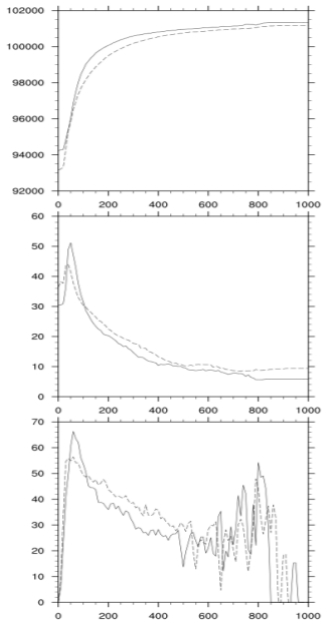

Figure 11 Azimuthally averaged MSLP (upper) model 10m wind speed (middle) and the 10-m wind speed derived from the cyclostrophic relation using the model MSLP (lower) in FA-adv (dashed) and FA (solid)

This radial distribution of the MSLP affects the pressure gradient $\frac{\partial P}{\partial r}$ and hence affects the tangential wind speed V. The tangential wind calculated according to the cyclostrophic relation is shown in the bottom panel of Figure 12. The model 10-m wind speed is plotted in the middle panel of Figure 12. We can see that although the magnitude of the tangential wind speeds calculated from the cyclostrophic wind relationship is higher than

the model output 10-m wind speed (meaning the model 10-m wind speed did not entirely follow the cyclostrophic wind), their patterns within 500 km distance from the vortex center resembled each other very well: they both have a weaker maximum wind speed in FA-adv but stronger in general for most of the radial distance for r > 100km. Note that the cyclostrophic wind relationship is not valid for the regions further away from the vortex center (r>500km) where the geostrophic wind relation probably takes over as the main balance.

Other sensitivity experiments using FA-adv and FA, as mentioned in Section 3, include (1) no diabatic heating in microphysics (2) no condensation in microphysics (3) no physics with all schemes shut down (4) zero cloud optical depth (COD) (5) no radiation (6) no cumulus. A significant finding from these sensitivity experiments is that when the diabatic heating associated with microphysics (heating due to phase change) is turned off or when the condensation process is turned off, the difference between the forecasted storm sizes for FA-adv and FA was largely eliminated. This confirms that the difference in the cloud water and its condensation due to the different advection methods (FA vs. FA-adv) is the main reason for the different forecasted storm sizes. In the experiments that looked at the impacts of cloud optical depth, radiation and cumulus processes, the difference between the forecasted storm sizes for FA and FA-adv always existed, suggesting they are not the main responsible factors.

6. Conclusion

The advection of the total condensate in the FA scheme seems to overestimate the upward advection of low-level rainwater and underestimate that of the cloud water. The separate advection of hydrometeors in the FA-adv scheme, in theory, corrected this problem, which leads to differences between the forecasted microphysics fields and TC dynamics for these two schemes. All the differences originated from the larger upward advection of cloud water associated with FA-adv, which continuously turns into ice and eventually into snow and rainwater. More importantly, the continuous source of cloud water also causes phase changes and thus the associated diabatic heating. The larger diabatic heating in FA-adv affects the dynamics of the simulated TC by importing more angular momentum. The radial pattern of the azimuthally averaged extra diabatic heating in FA-adv causes the MSLP to adjust in a manner that, according to the cyclostrophic balance relation, leads to a weaker maximum wind speed. The larger imported angular momentum in FA-adv, therefore, caused the storm's size to expand, and the wind speed to increase in the areas further away from the vortex center. Therefore, although the overall 10-m wind speed is stronger in FA-adv, its maximum 10-m wind is weaker than that in FA.

Although in theory the separate advection of hydrometeors in FA-adv is more realistic than the advection of total condensate in FA, this evaluation showed that FA-adv forecasted much larger storms than FA and the observed TCs, and therefore degraded the HWRF performance. It should be noted that HWRF, like other NWP models, is a very complex system, and the tuning in other parts of the model system could have masked the errors introduced by the total condensate advection. That is why in this study we focused on understanding the mechanisms that are responsible for the differences between the FA and FA-adv forecasts, instead of seeking to

improve the HWRF performance with FA-adv. Future work is needed to identify those tunings so that the separate hydrometeors advection can achieve better forecast performance.

7. Reference list

- Aligo, E., Ferrier, B., Carley, J., Rogers, E., Pyle, M., Weiss, S.J., Jirak, I.L., 2014. Modified microphysics for use in high-resolution NAM forecasts, in: Proc. 27th Conf. on Severe Local Storms. Madison, WI.
- Ferrier, B.S., 2005. An efficient mixed-phase cloud and precipitation scheme for use in operational NWP models. EOS Trans. AGU, Jt. Assem. Suppl. 86, A42-02.
- Ferrier, B.S., 1994. A double-moment multiple-phase four-class bulk ice scheme. Part I: Description. Journal of the Atmospheric Sciences 51, 249–280.
- Fovell, R.G., Su, H., 2007. Impact of cloud microphysics on hurricane track forecasts. Geophys. Res. Lett. 34, L24810.
- Pattnaik, S., Krishnamurti, T.N., 2007a. Impact of cloud microphysical processes on hurricane intensity, part 1: Control run. Meteorology and Atmospheric Physics 97, 117–126.
- Pattnaik, S., Krishnamurti, T.N., 2007b. Impact of cloud microphysical processes on hurricane intensity, part 2: Sensitivity experiments. Meteorology and Atmospheric Physics 97, 127–147.
- Skamarock, W.C., Klemp, J.B., Dudhia, J., Gill, D.O., Barker, D.M., Duda, M.G., Huang, X.Y., Wang, W., Powers, J.G., 2008. A description of the Advanced Research WRF Version 3. NCAR Technical Note, NCAR/TN-475+STR 113.
- Biswas, M., Bernardet, L., Abarca, S., Ginis, I., Grell, E., Kalina, E., Kwon, Y., Liu, B., Liu, Q., Marchok, T., Mehra, A., Newman, K., Sheinin, D., Sippel, J., Subramanian, S., Tallapragada, V., Thomas, B., Tong, M., Trahan, S., Wang, W., Yablonsky, R., Zhang, X., Zhang, Z., 2018. Hurricane weather research and forecasting (HWRF) model: 2017 scientific documentation. NCAR Technical Notes NCAR/TN-544+STR
- Thompson, G., Field, P.R., Rasmussen, R.M., Hall, W.D., 2008. Explicit forecasts of winter precipitation using an improved bulk microphysics scheme. Part II: Implementation of a new snow parameterization. Monthly Weather Review 136, 5095–5115.
- Zhu, T., Zhang, D.-L., 2006. Numerical Simulation of Hurricane Bonnie (1998). Part II: Sensitivity to Varying Cloud Microphysical Processes. J. Atmos. Sci. 63, 109–126.